

On the lattice dynamics of metallic hydrogen and other Coulomb systems

Autor(en): **Beck, H. / Straus, D.**

Objektyp: **Article**

Zeitschrift: **Helvetica Physica Acta**

Band (Jahr): **48 (1975)**

Heft 5-6

PDF erstellt am: **10.08.2024**

Persistenter Link: <https://doi.org/10.5169/seals-114691>

Nutzungsbedingungen

Die ETH-Bibliothek ist Anbieterin der digitalisierten Zeitschriften. Sie besitzt keine Urheberrechte an den Inhalten der Zeitschriften. Die Rechte liegen in der Regel bei den Herausgebern.

Die auf der Plattform e-periodica veröffentlichten Dokumente stehen für nicht-kommerzielle Zwecke in Lehre und Forschung sowie für die private Nutzung frei zur Verfügung. Einzelne Dateien oder Ausdrucke aus diesem Angebot können zusammen mit diesen Nutzungsbedingungen und den korrekten Herkunftsbezeichnungen weitergegeben werden.

Das Veröffentlichen von Bildern in Print- und Online-Publikationen ist nur mit vorheriger Genehmigung der Rechteinhaber erlaubt. Die systematische Speicherung von Teilen des elektronischen Angebots auf anderen Servern bedarf ebenfalls des schriftlichen Einverständnisses der Rechteinhaber.

Haftungsausschluss

Alle Angaben erfolgen ohne Gewähr für Vollständigkeit oder Richtigkeit. Es wird keine Haftung übernommen für Schäden durch die Verwendung von Informationen aus diesem Online-Angebot oder durch das Fehlen von Informationen. Dies gilt auch für Inhalte Dritter, die über dieses Angebot zugänglich sind.

On the Lattice Dynamics of Metallic Hydrogen and Other Coulomb Systems

by **H. Beck**¹⁾

IBM Zurich Research Laboratory, 8803 Rüschlikon, Switzerland

and **D. Straus**²⁾

Laboratory of Atomic and Solid-State Physics, Cornell University,
Ithaca, N.Y. 14853, USA

(14. VII. 75)

Abstract. Numerical results for the phonon spectra of metallic hydrogen and other Coulomb systems in cubic lattices are presented. In second order in the electron-ion interaction the behavior of the dielectric function of the interacting electron gas for arguments around $2k_F$ leads to drastic Kohn anomalies and even to imaginary phonon frequencies. Third-order band-structure corrections are also calculated. Furthermore the properties of self-consistent phonons and the validity of the adiabatic approximation are discussed.

I. Introduction

Since Wigner and Huntington's original work [1], there has been a large effort devoted to the study of metallic hydrogen. Considerable demands are put on the experimentalist, who must produce the very high pressure (presumably a few megabars) necessary to produce the metallic phase. There have been two recent reports of fabrication of the metal, one by implosion techniques [2] and the other by static means [3]. Theoretical questions of interest include the prediction of the transition pressure, the possibility of a metastable metallic form at zero pressure, and the determination of the structure of the metal as a function of pressure. Also of interest are the transport properties, such as its conductivity, and in particular the determination of the transition temperature to a superconducting state.

The understanding of the structure of the metal demands very accurate evaluation of the static and dynamic energies of a wide range of lattice structures, and of the liquid state. There has been a fair amount of work on the comparison of static structural energies in the solid [4–11], all of it based on perturbation theory in the electron-proton interaction. To improve upon the accuracy of the *static* energies reported in these papers would involve very extensive numerical work. That is not the purpose of this work. Rather, we look in some detail at the *dynamics* of various structures, a less well-documented area. We are concerned with the origin of various dynamical structural instabilities, and their relation to structural differences in static energies.

¹⁾ IBM Post-doctoral Fellow from the Theoretical Physics Institute of the University, Zurich, Switzerland.

²⁾ Work supported by US National Science Foundation (Contract DMR 74-23494) and in part by NASA (Contract NGR-33-010-188).

These instabilities manifest themselves in the occurrence of negative eigenvalues of the harmonic dynamical matrix for some points of the Brillouin zone. We will trace these instabilities to the rapid variation of the dielectric function of the interacting electron gas at $k = 2k_F$, and hence connect them with the well-known criteria for static stability (e.g., the Hume-Rothery rules (see Refs. [12] and [13])). Another concern will be the effect on these instabilities of going beyond the simplest treatment of phonons in metals. By the latter, we mean calculating the dynamical matrix in the harmonic, adiabatic approximation, including only second order in the electron-ion interaction. We do this by including third order in the electron-ion coupling and corrections to adiabaticity in the harmonic dynamical matrix, and by examining work that has been done with the self-consistent harmonic theory [14].

The behavior of the dynamical matrix for hydrogen will be compared to that for other Coulomb systems, which we now introduce.

Metallic hydrogen is thought to account for a large part of the matter of the solar system, virtually all of it residing in Jupiter and Saturn [15]. The presence of helium in Jupiter, along with the extremely high pressure at its center, suggests that the helium too may be metallic here. [By metallic helium we envisage a collection of doubly-charged point ions (alpha particles) immersed in a responding electron gas of appropriate density³.] Now the properties of hydrogen-helium mixtures may be crucial for understanding Jupiter's production of energy [16, 17], so that a calculation of the properties of hydrogen-helium mixtures ('alloys') becomes of interest.

It was in fact just such a calculation (i.e., the phase separation curve of these alloys) which motivated the authors to embark upon the present study. If we assume the alloys are completely disordered, it can be shown that all the terms *which depend on structure* in the static energy and in the dynamics can be arrived at by replacing each ion with one of *average charge*. Thus we would view a 50% hydrogen (by number) alloy as a system of point ions of charge +1.5 and mass $\sqrt{M_H M_{He}}$ immersed in a responding electron gas. The derivation of these statements will be given in a subsequent paper.

In the following section, we present the basic theory of the dynamical matrix of Coulomb systems in the harmonic approximation. The electron-proton coupling will be taken into account up to third order, and we will discuss the adequacy of the adiabatic approximation. In Section III, we discuss the numerical results for some phonon spectra (for cubic structures) and the behavior and origin of the instabilities. We try to assess the importance of these findings in the Conclusion.

II. Theory

The usual pseudopotential theory of simple metals, as described in Refs. [18, 19] starts from the Hamiltonian

$$H_p = \sum_n \frac{1}{2M_n} \mathbf{P}_n^2 + \frac{1}{2} \sum_{nn'} W(\mathbf{R}_n - \mathbf{R}_{n'}) \quad (\text{II.1a})$$

$$H_e = \sum_i \frac{1}{2m} \mathbf{p}_i^2 + \frac{1}{2} \sum_{ij}' \frac{e^2}{|\mathbf{r}_i - \mathbf{r}_j|} \quad (\text{II.1b})$$

³) We introduce helium as a metal for the sake of clarity. But it should be stressed that our calculations in the framework of perturbation theory are in principle valid at these densities, whatever the conduction properties of the helium.

$$H_1 = - \sum_{in} V(\mathbf{r}_i - \mathbf{R}_n). \quad (\text{II.1c})$$

Here \mathbf{P}_n and \mathbf{R}_n are the momenta and coordinates of the ions with mass M_n , respectively, which interact through the pair potential W , whereas \mathbf{p}_i and \mathbf{r}_i describe the momenta and positions of the electrons of mass m . The pseudopotential V acts between ion and (conduction) electrons. In the case of hydrogen and helium, both potentials are given by the Coulomb interaction, e.g.,

$$W(\mathbf{R}_n - \mathbf{R}_{n'}) = \frac{Z_n Z_{n'} e^2}{|\mathbf{R}_n - \mathbf{R}_{n'}|}, \quad (\text{II.2})$$

Z_n giving the charge at lattice site n ($1 \leq Z_n \leq 2$). Thus the usual uncertainty about the pseudopotential is absent here. The aim now is to eliminate the electronic degrees of freedom and thus to derive an effective Hamiltonian \bar{H}_p for the ions alone. This is easily done (at least formally) in the adiabatic approximation which, for this elimination procedure, treats the ionic position variables as c numbers. The electrons follow the much slower motions of the protons instantaneously. We can write the partition function as

$$Z(\beta) = \text{Tr}_p \text{Tr}_{el} e^{-\beta(H_p + H_e + H_1)} \equiv \text{Tr}_p e^{-\beta \bar{H}_p}, \quad (\text{II.3})$$

where Tr_p and Tr_{el} denote traces over proton and electron variables, respectively. \bar{H}_p defined by (II.3), can be written as a power series in the electron-proton interaction (V_{ep}):

$$\bar{H}_p = \tilde{H}_p + F_{el} + \sum_{\nu=2}^{\infty} \frac{1}{\nu!} \bar{H}_p^{(\nu)}, \quad (\text{II.4})$$

F_{el} is the free energy of the interacting electron gas alone (usually taken at $T = 0$). \tilde{H}_p results from the original H_p by adding a term which represents the interaction of the protons with a uniform background of negative charge (Madelung energy). Finally $\bar{H}_p^{(\nu)}$ is of the form

$$\bar{H}_p^{(\nu)} \propto \sum_{n_1 \dots n_\nu} \int d^3 r_1 \dots d^3 r_\nu V(\mathbf{r}_1 - \mathbf{R}_{n_1}) \dots V(\mathbf{r}_\nu - \mathbf{R}_{n_\nu}) \langle \delta\rho(\mathbf{r}_1) \dots \delta\rho(\mathbf{r}_\nu) \rangle_{el}. \quad (\text{II.5})$$

It is a ν -body operator as far as the proton variables are concerned and involves ν -fold density correlation functions of the interacting electron gas. In $\delta\rho(\mathbf{r})$ the uniform component $\langle \rho \rangle$ of the electronic density must be subtracted out.

Following the usual methods of lattice dynamics, the proton coordinates are resolved into equilibrium positions and deviations $\mathbf{U}_{n\sigma}$:

$$\mathbf{R}_{n\sigma}(t) = \mathbf{X}_{n\sigma} + \mathbf{U}_{n\sigma}(t); \quad \mathbf{X}_{n\sigma} = \mathbf{X}_n + \mathbf{b}_\sigma, \quad (\text{II.6})$$

where n identifies the unit cell at position \mathbf{X}_n , and \mathbf{b}_σ points to the different protons in each unit cell. Thus \bar{H}_p in (II.4) is used in two ways: First set all $\mathbf{U}_{n\sigma}$ to zero. The value $\bar{H}_p(\{\mathbf{R}_{n\sigma}\} = \{\mathbf{X}_{n\sigma}\})$ is the static energy of the system

$$E_{\text{STAT}} = F_{el} + E_M + E_{\text{BS}}. \quad (\text{II.7})$$

E_M denotes the Madelung energy and E_{BS} summarizes the 'band-structure' corrections involved in including the electron response to second and higher order in V_{ep} . For investigating the dynamic properties of the metal \bar{H}_p is then expanded in powers of U_{ns} . Truncating the expansion after the quadratic term (the linear term must vanish) we obtain the harmonic dynamical matrix, which is given explicitly below. It consists of the Coulomb part $D^{(c)}$, describing oscillations of the protons in a uniform negative background, and various band-structure corrections [e.g. $D^{(2)}$]. The Coulomb part must be calculated by means of Ewald's technique [20–22] which is designed to handle the long-range nature of the Coulomb interaction. This technique introduces a parameter λ into the dynamical matrix in such a way that the latter must be independent of it, even though this is not obvious from the resulting formulae. We obtain

$$D_{ij,\sigma\sigma'}(\mathbf{q}) = D_{ij,\sigma\sigma'}^{(c)}(\mathbf{q}) + D_{ij,\sigma\sigma'}^{(2)}(\mathbf{q}) + D_{ij,\sigma\sigma'}^{(3)}(\mathbf{q}) + \dots, \quad (\text{II.8})$$

where

$$\begin{aligned} D_{ij,\sigma\sigma'}(\mathbf{q}) = (\omega_p^2)_{\sigma\sigma'} \left\{ \sum_{\mathbf{K}} \frac{(K+q)_i(K+q)_j}{(\mathbf{K}+\mathbf{q})^2} e^{-(\mathbf{K}+\mathbf{q})^2/\lambda^2} e^{i\mathbf{K}\cdot(\mathbf{b}_\sigma-\mathbf{b}_{\sigma'})} \right. \\ - \delta_{\sigma\sigma'} \sum_{\mathbf{K}}' \frac{K_i K_j}{K^2} \sum_{\sigma''} \frac{Z_{\sigma''}}{Z_\sigma} e^{-\mathbf{K}^2/\lambda^2} e^{i\mathbf{K}\cdot(\mathbf{b}_\sigma-\mathbf{b}_{\sigma''})} \\ - \frac{\Omega_c}{\pi a_L^3} \left[\sum_n B_{ij}(\mathbf{b}_\sigma - \mathbf{b}_{\sigma'} - \mathbf{X}_n) e^{i\mathbf{q}\cdot(\mathbf{b}_\sigma-\mathbf{b}_{\sigma'}-\mathbf{X}_n)} \right. \\ \left. \left. - \delta_{\sigma\sigma'} \sum_n \sum_{\sigma''} \frac{Z_{\sigma''}}{Z_\sigma} B_{ij}(\mathbf{b}_\sigma - \mathbf{b}_{\sigma''} - \mathbf{X}_n) \right] \right\}; \quad (\text{II.9}) \end{aligned}$$

$$\begin{aligned} D_{ij,\sigma\sigma'}^{(2)}(\mathbf{q}) = (\omega_p^2)_{\sigma\sigma'} \left[\sum_{\mathbf{K}} \frac{(K+q)_i(K+q)_j}{(\mathbf{K}+\mathbf{q})^2} e^{i\mathbf{K}\cdot(\mathbf{b}_\sigma-\mathbf{b}_{\sigma'})} \left(\frac{1}{\epsilon(\mathbf{K}+\mathbf{q})} - 1 \right) \right. \\ \left. - \delta_{\sigma\sigma'} \sum_{\mathbf{K}} \frac{K_i K_j}{K^2} \sum_{\sigma''} \frac{Z_{\sigma''}}{Z_\sigma} e^{i\mathbf{K}\cdot(\mathbf{b}_\sigma-\mathbf{b}_{\sigma''})} \left(\frac{1}{\epsilon(K)} - 1 \right) \right]. \quad (\text{II.10}) \end{aligned}$$

Here the Cartesian indices i and j run from 1 to 3, whereas $\sigma = 1 \dots s$ numbers the s possible vectors \mathbf{b}_σ in each cell. The cell has volume Ω_c , and a_L refers to the length of the conventional cube side for FCC and BCC lattices, and to the lattice constant for SC lattices. The sums over \mathbf{K} run over the reciprocal lattice, and a prime over the sum denotes omission of $\mathbf{K} = \mathbf{0}$. The common factor is a 'plasma frequency matrix'

$$(\omega_p^2)_{\sigma\sigma'} = \frac{4\pi e^2 Z_\sigma Z_{\sigma'}}{\Omega_c (M_\sigma M_{\sigma'})^{1/2}}. \quad (\text{II.11})$$

This depends on the charges Z_σ and the masses M_σ of the basis ions. The function B_{ij} is given by

$$B_{ij}(\underline{x}) = \frac{x_i x_j}{x^2} A(|\underline{x}|) + \delta_{ij} B(|\underline{x}|) \quad (\text{II.12})$$

with

$$A(x) = 6 \frac{1 - \Phi(x\lambda\pi/2)}{x^3} + 2\lambda\sqrt{\pi} \frac{e^{-(\lambda\pi x/2)^2}}{x^2} \left(3 + \frac{(\lambda\pi x)^2}{2} \right) \quad (\text{II.13a})$$

$$B(x) = - \left[2 \frac{1 - \Phi(x\lambda\pi/2)}{x^3} + 2\lambda\sqrt{\pi} \frac{e^{-(\lambda\pi x/2)^2}}{x^2} \right]. \quad (\text{II.13b})$$

Φ being the error function. For $x = 0$ we define $A(x) = B(x) = 0$. Finally $\epsilon(k)$ arising in (II. 10) is the dielectric function of the interacting electron gas. There is some controversy about which form of $\epsilon(k)$ given in the literature is the best. Stoll et al. [7] have shown that the choice of ϵ can influence the equation of state appreciably, but mainly at low densities. The subsequent analysis depends only on a basic property of ϵ common to all the various approximations currently in use [23–25]. This is the logarithmic divergence in the derivative of ϵ at $k = 2k_F$ already inherent in the Hartree or Lindhard form. We work with what is termed the ‘Hubbard-Geldart-Vosco’ form [26]. In the reduced variable $\eta \equiv k/2k_F$, it is

$$\epsilon(\eta) = 1 + \frac{(A/\eta^2)F(\eta)}{1 - \frac{AF(\eta)}{2\eta^2 + g}} \quad (\text{II.14})$$

with

$$A = \frac{r_s}{2\pi} \left(\frac{4}{9\pi} \right)^{1/3}$$

$$g = \left[1 + 0.031 \left(\frac{4}{9\pi} \right)^{1/3} \frac{\pi}{2} r_s \right]^{-1}$$

and

$$F(\eta) = 1 + \frac{(1 - \eta^2)}{2\eta} \log \left| \frac{1 + \eta}{1 - \eta} \right|, \quad (\text{II.15})$$

where r_s characterizes the density of the electron gas. A sphere of volume $\frac{4}{3}\pi r_s^3$ (in atomic units $\hbar = e = m = 1$) encloses the volume per electron, k_F is the Fermi wave vector⁴), and the factor g is weakly density dependent. It is chosen so that the compressibility calculated from $\epsilon(k)$ coincides with the second derivative of the electron-gas energy with respect to density. In this form of ϵ the latter is obtained from the Nozieres–Pines interpolation formula [27].

For the sake of simplicity the third-order part of the dynamical matrix is only given for a Bravais lattice with charge Z (see also Ref. [28]):

$$D_{ij}^{(3)}(\mathbf{q}) = -\omega_p^2 r_s^2 \frac{2}{3\pi^2} \left(\frac{4}{9\pi} \right)^{2/3} \frac{1}{Z^3} [\Psi(\mathbf{q}) - \Psi(\mathbf{0})] \quad (\text{II.16})$$

with

$$\Psi(\mathbf{q}) = \sum_{\mathbf{K}, \mathbf{K}'} \frac{(q + K)_i (q + K')_j}{(\mathbf{q} + \mathbf{K})^2 (\mathbf{q} + \mathbf{K}')^2 (\mathbf{K} - \mathbf{K}')^2} \cdot \frac{\tilde{Z}(\mathbf{q} + \mathbf{K}, -\mathbf{q} - \mathbf{K}', \mathbf{K}' - \mathbf{K})}{\epsilon(\mathbf{q} + \mathbf{K})\epsilon(\mathbf{q} + \mathbf{K}')\epsilon(\mathbf{K} - \mathbf{K}')} \quad (\text{II.17})$$

In the double sum over \mathbf{K} and \mathbf{K}' terms which would yield vanishing denominators are to be omitted. The function \tilde{Z} is equal to the three-pole $\Lambda^{(3)}$ used in Ref. [28] and has been calculated by Lloyd and Sholl [29]. The overall minus sign in equation (II. 16),

⁴) $k_F^3 \equiv 3\pi^2 n_e$, where n_e is the number density of electrons.

due to three powers of the attractive electron-ion interaction, may be misleading. The quantity in the brackets may be negative. It should also be remarked here that the triple-density correlation function of the electron gas entering (II. 17), i.e., the function \tilde{Z} divided by the three dielectric functions, is a Hartree-like approximation. This is in contrast to the form of $D^{(2)}$ in (II.10), which is formally exact, since the dielectric function is directly related to the density-density correlation function. The three-pole \tilde{Z} becomes singular for certain values of the arguments. Hammerberg [10] has developed a method for handling this type of singularity. It essentially involves taking into account some features of the true band structure. This is done by incorporating effects of the higher orders in V_{ep} into the third-order term. We shall, however, not go into these problems, since we only wish to estimate the effect of $D^{(3)}$ on the phonon spectrum in a rough way.

Equations (II.8) to (II.10) are valid for any lattice of metallic H or He, or completely ordered alloys of the two. Random alloys can be considered in the 'virtual-crystal' approximation by using the same formulae with each Z_σ replaced by Z^* , the average charge.

Whereas the third-order term (II.16) involves three-body forces, it is possible to derive the dynamical matrix at second order in V_{ep} from an effective pair potential, as is usually done in the framework of lattice dynamics in insulators. It is of the form

$$V(\mathbf{r}) = \frac{4\pi e^2}{\Omega} \sum_{\mathbf{q} \neq 0} \frac{e^{i\mathbf{q} \cdot \mathbf{r}}}{q^2 \epsilon(q)}, \quad (\text{II.18})$$

where Ω is the volume of the system.

In practice, due to convergence problems, the 'induced part'

$$V_{\text{ind}}(\mathbf{r}) = \frac{4\pi e^2}{\Omega} \sum_{\mathbf{q} \neq 0} \frac{e^{i\mathbf{q} \cdot \mathbf{r}}}{q^2} \left[\frac{1}{\epsilon(q)} - 1 \right] \quad (\text{II.19})$$

is calculated separately and then added to the bare Coulomb repulsion.

Recently Caron [14] has calculated self-consistent phonon frequencies for FCC metallic hydrogen. This method is well-known in the theory of quantum crystals [30] and is equivalent to finding that harmonic trial Hamiltonian which minimizes the free energy. The part of the self-consistent dynamical matrix which is of second order in V_{ep} can again be derived from an (effective) pair potential. The value of this pair potential for a pair of ions separated by a vector \mathbf{X}_n is found by a convolution of the bare potential with the (self-consistently calculated) static pair correlation function of the two particles

$$\tilde{V}_n(\mathbf{X}_n) = \int d^3r V(\mathbf{r}) g_n(\mathbf{r}, \mathbf{X}_n) \quad (\text{II.20})$$

with

$$g_n(\mathbf{r}, \mathbf{X}_n) = \langle \delta[\mathbf{r} - (\mathbf{X}_n + \mathbf{U}_n) - \mathbf{U}_0] \rangle. \quad (\text{II.21})$$

The values $\tilde{V}_n(\mathbf{X}_n)$ can be continued to a function $\tilde{V}_n(\mathbf{X})$ of the continuous variable \mathbf{X} . Since g_n is a Gaussian in the self-consistent harmonic approximation we find

$$\tilde{V}_n(\mathbf{X}) = \frac{4\pi e^2}{\Omega} \sum_{\mathbf{q} \neq 0} \frac{e^{i\mathbf{q} \cdot \mathbf{X}}}{q^2 \epsilon(q)} e^{-q_i q_j G_{ij}^{(n)}}. \quad (\text{II.22})$$

The 'width tensor' involves the displacement correlation function of the two particles

$$G_{ij}(n) = \langle U_i(n)U_j(n) \rangle - \langle U_i(n)U_j(0) \rangle. \quad (\text{II.23})$$

The adiabatic approximation can easily be avoided, at least in the harmonic treatment, including only second order in V_{ep} . Baym [31] has derived an expression for a frequency-dependent dynamical matrix $D_{ij,\sigma\sigma'}(\mathbf{q}, z)$ which is formally identical to (II.10), except that $\epsilon(\mathbf{K} + \mathbf{q})$ has to be replaced by the frequency-dependent dielectric function $\epsilon(\mathbf{K} + \mathbf{q}, z)$. [The term $1/\epsilon(K)$ in the second part of (II.10) remains unchanged.] Then Dyson's equation for the phonon propagator $G_{ij}(\mathbf{q}, z)$ reads (for brevity omitting the indices σ, σ')

$$\sum_i [z^2 \delta_{ii} - D_{ii}(\mathbf{q}, z)] G_{ij}(\mathbf{q}, z) = \delta_{ij}. \quad (\text{II.24})$$

D is diagonalized for each value of z , yielding

$$G(\mathbf{q}\lambda, z) = [z^2 - D(\mathbf{q}\lambda, z)]^{-1} \quad (\text{II.25})$$

for all polarizations λ . If $D(\mathbf{q}\lambda, z = \Omega + i\delta)$ has an imaginary part the phonons acquire a finite spectral width. The interpretation of (II.25) will be discussed at the end of Section III.

III. Phonon Spectra and Dynamic Instabilities

Here we present the phonon spectra for cubic lattices. Figures 1 to 3 show phonon spectra of FCC metallic hydrogen calculated in various approximations. They strongly depend on r_s ⁵⁾, i.e., on density or pressure. According to Figure 1, the harmonic frequencies (to second order in V_{ep}) are all real for $r_s \leq 1$. At $r_s = 1.3$, the frequencies of transverse vibrations were imaginary in some parts of the zone, signaling a dynamic instability. BCC and SC lattices have instabilities that manifest themselves over a much wider density range. Only for very high density are these lattices harmonically stable (see Table I).

Similar things happen in calculations for insulating crystals. In solid He all harmonic frequencies are imaginary [32]. There the apparent instability (solid He does exist!) is solely due to an inadequate theoretical treatment of the pair potential. Owing to zero-point vibrations nearest neighbors are so far apart that the second derivative of the pair potential (evaluated at the equilibrium distance) is negative. Suitable renormalization procedures [32] lead to an effective pair potential yielding real phonon frequencies. (The minimum of this effective pair potential is shifted to larger distances.) Our pair potential, (II.18), which enters the second-order phonon calculations, is plotted in Figure 4 for various r_s values. Near-neighbor distances for the FCC lattice are also shown. It is clear that the instabilities in Figure 1b are not of the same origin as sketched for the insulating quantum crystal above. The nearest neighbors in this case even lie on the 'core' of the Coulomb potential, and the neighbors further out lie in valleys or on hills of $V(\mathbf{r})$, seemingly at random.

⁵⁾ Metallic hydrogen has extremely high electronic densities. We expect $r_s \approx 1.6$ (see Ref. [8]) for the (possibly metastable) zero pressure phase and $r_s \approx 1.3$ at the transition pressure between molecular and metallic H, which is probably about 3–4 Mbar. He will not become metallic unless $r_s \lesssim 0.8$.

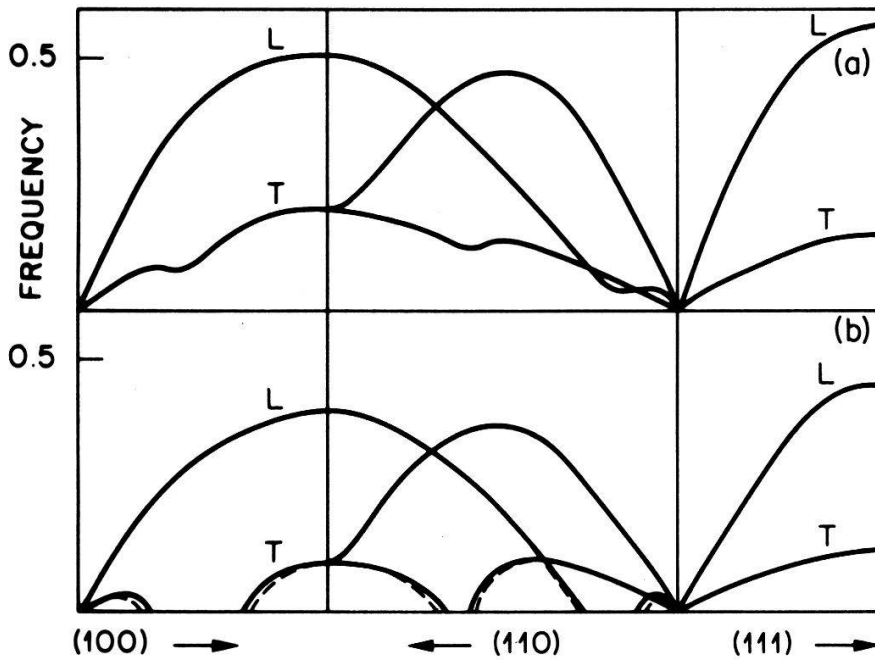


Figure 1

Full lines: harmonic, adiabatic phonon frequencies for FCC metallic hydrogen (in units of the plasma frequency [see footnote 6]), including second order in V_{ep} . Fig. 1a: $r_s = 1$, Fig. 1b: $r_s = 1.3$. In the missing parts of the curves for the lowest transverse branch the frequencies would be imaginary. (L and T denote longitudinal and transverse, respectively.) The spectra are shown for three symmetry directions:

$$\begin{aligned} (100): \mathbf{q} &= 2\pi/a_L \cdot (\xi, 0, 0) & 0 \leq \xi \leq 1 \\ (110): \mathbf{q} &= 2\pi/a_L \cdot (\xi, \xi, 0) & 0 \leq \xi \leq 1 \\ (111): \mathbf{q} &= 2\pi/a_L \cdot (\xi, \xi, \xi) & 0 \leq \xi \leq 0.5 \end{aligned}$$

The dashed curves indicate corrections due to the non-adiabatic treatment explained in the text.

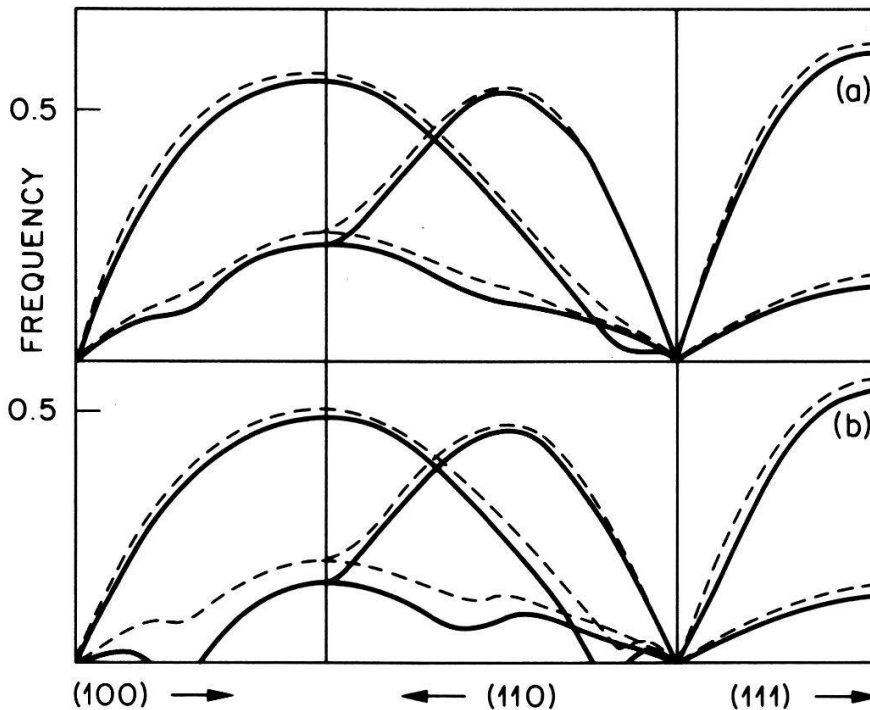


Figure 2

Full lines: harmonic, adiabatic frequencies for FCC hydrogen including the third-order term (II.16), Fig. 2a: $r_s = 0.8$, Fig. 2b: $r_s = 1$. For comparison the second-order frequencies are shown by dashed curves.

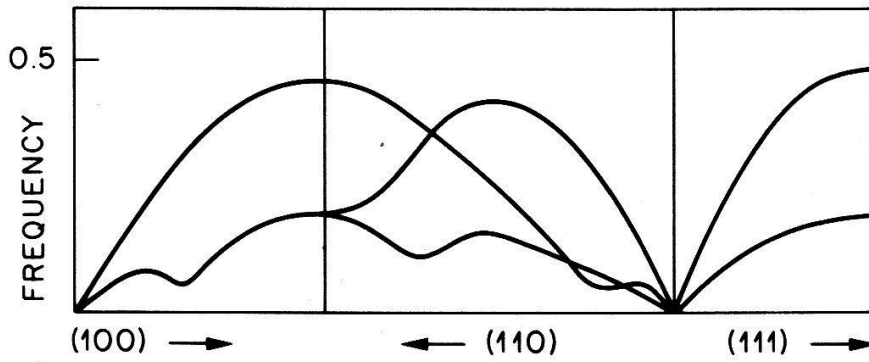


Figure 3
Self-consistent harmonic spectrum for $r_s = 1.3$, taken from Caron's work, Ref. [14].

A closer inspection of Figure 1 shows that in those regions of q space where there is an instability at $r_s = 1.3$, there is already a dip in the curve at $r_s = 1.0$. This is a Kohn anomaly [33], which for large values of r_s is so strong that it drives the transverse frequency to zero. To find the origin of this instability we examine the dynamical matrix along a symmetry direction in q space [$\mathbf{q} = 2\pi/a_L(\xi, 0, 0)$]. Here the matrix is diagonal and we concentrate on the (doubly degenerate) value $D_{yy} = D_{zz}$ for transverse phonons. The Coulomb part $D_{yy}^{(c)}$ is always positive, so evidently for some values of \mathbf{q} , $D_{yy}^{(2)}(\mathbf{q})$ is excessively large and negative. In fact this behavior of $D^{(2)}(\mathbf{q})$ can be tied to a set of reciprocal lattice vectors in the sum of (II.10). This set, in this case, is $\mathbf{K} = 2\pi/a_L(-1, \pm 1, \pm 1)$. Near $\xi = 0$, $|\mathbf{q} + \mathbf{K}| > 2k_F$ so that $(1/\epsilon - 1)$ is relatively small. However, as ξ increases to 0.4, $|\mathbf{q} + \mathbf{K}|$ becomes just *less* than $2k_F$. Here $(1/\epsilon - 1)$ suddenly becomes much more negative. Thus for a relatively small change in \mathbf{q} , $D_{yy}^{(2)}(\mathbf{q})$ has become markedly more negative. In Figure 1a we see the resulting Kohn anomaly at $\xi = 0.4$. Since the function $(1/\epsilon - 1)$ appearing in (II.10) is roughly proportional to r_s , the value of r_s will determine whether the phonon frequencies actually become negative (Fig. 1b), or whether there is only a Kohn anomaly (Fig. 1a).

The essential features of the above example are the following: We have a \mathbf{K} vector lying just *outside* and close to the sphere of radius $2k_F$, so that there is a vector \mathbf{q} for which $|\mathbf{K} + \mathbf{q}|$ is just *inside* the sphere. The rapid variation of $(1/\epsilon - 1)$ at $2k_F$ leads, in the above situation, to a rapid increase in the (negative) contribution $D^{(2)}(\mathbf{q})$ as \mathbf{q} increases. Thus the key feature is the behavior of $\epsilon(q)$ at $2k_F$. Ashcroft and Stroud [13]

Table I

Ranges of r_s where random alloys with average charge Z per lattice site show stable (unstable) harmonic, second-order phonons in virtual crystal approximation. Only the interval $0.6 \leq r_s \leq 1.5$ has been considered.

Z	BCC		FCC	
	stable	unstable	stable	unstable
1.0	—	$r_s > 0.6$	$0.6 < r_s < 1$	$1 < r_s < 1.5$
1.2	—	$r_s > 0.6$	—	$r_s > 0.6$
1.4	—	$r_s > 0.6$	$0.6 < r_s < 1.1$	$r_s > 1.1$
1.6	$0.6 < r_s < 1.5$	—	—	$r_s > 0.6$
1.8	$0.6 < r_s < 1.5$	—	—	$r_s > 0.6$
2.0	$0.6 < r_s < 1.5$	—	—	$r_s > 0.6$

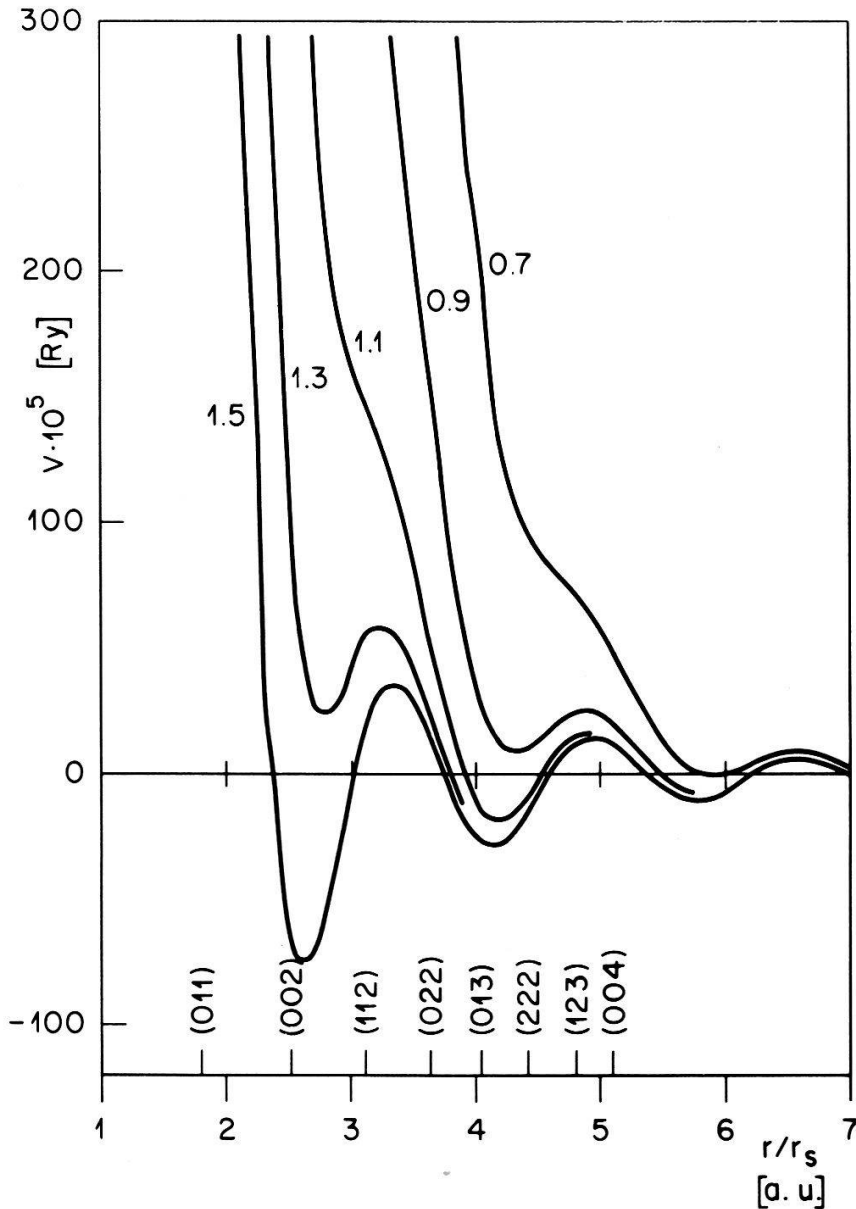


Figure 4
Effective pair potential $V(r)$ according to (II.18) plotted as a function of the reduced distance r/r_s (measured in atomic units⁶). Each curve is labelled by the corresponding r_s value. On the bottom line the locations of the first few nearest neighbors for an FCC lattice are marked.

have shown that this behavior is responsible for the Hume-Rothery rules [12] and in general plays a large role in the (second-order) determination of static structural stability. (We will return to this point.)

The opposite situation, \mathbf{K} lying *inside* and close to the $2k_F$ sphere, does not have the same effect. As $|\mathbf{q}|$ increases, so that $|\mathbf{q} + \mathbf{K}|$ passes through the $2k_F$ sphere from the inside, the contribution $D_{yy}^{(2)}(\mathbf{q})$ becomes much smaller. So if $D_{yy}^{(c)} + D_{yy}^{(2)} > 0$ for \mathbf{q} near zero, the sum will remain positive as \mathbf{q} increases.

This argument can be used to understand the dynamic instability of disordered alloys. For here, just as in the consideration of the Hume-Rothery rules, the relationship

⁶) The atomic unit of length is $5.29 \cdot 10^{-9}$ cm. The plasma frequency, according to (II.11), for FCC hydrogen is $\hbar\omega_p = 8 \cdot 10^{-2}/r_s^{3/2}$ Ry, or $\omega_p = 2\pi \cdot 2.6 \cdot 10^{14}/r_s^{3/2}$ Hz.

Table II

Smallest reciprocal lattice vectors (in units of $2\pi/a_L$) and their magnitudes, as well as $2k_F$ in the same units for cubic lattices of various charges. The arrow marks where the nearest \mathbf{K} vector (011) for BCC goes inside the $2k_F$ sphere.

Lattice	\mathbf{K} vectors (and magnitude)	$2k_F$ for various Z					
		$Z = 1$	1.2	1.4	1.6	1.8	2
BCC	(011), (002), (112) 1.41 2 2.45	1.24	1.32	1.39 \uparrow	1.44	1.52	1.55
FCC	(111), (200), (220) 1.73 2 2.82	1.56	1.66	1.75	1.82	1.91	1.96

between the $2k_F$ sphere and any \mathbf{K} vector changes with Z^* , the average charge of an ion. From Table I we see that as Z increases from 1.0 to 2.0, the BCC lattice becomes harmonically stable very dramatically when Z lies between 1.4 and 1.6. Table II shows us the magnitude of $2k_F$ and the near-neighbor \mathbf{K} 's (in units of $2\pi/a_L$) for the BCC lattice as a function of Z . Note that the value of Z at which the nearest-neighbor \mathbf{K} vector passes *inside* the $2k_F$ sphere lies between 1.4 and 1.6. (See the arrow in Table II.) The trends in the FCC lattice as reported in Table I can also be well understood in terms of Table II and the above discussion, but here two sets of \mathbf{K} vectors are involved.

Let us now consider the interpretation of this instability (at second order in V_{ep}) in *real* space. Although only a rapid variation in $(1/\epsilon - 1)$ near $2k_F$ is needed to produce the instability, the electron-gas dielectric function has an actual logarithmic singularity in its derivative at $2k_F$. It is well known [34] that this leads to oscillatory behavior of the real-space pair potential $V(\mathbf{r})$, as $r \rightarrow \infty$ (see Fig. 4). The period of oscillation is $(\frac{1}{2}k_F)$, and the oscillations get more pronounced with higher r_s . Thus it is tempting to interpret the instabilities in real space as arising from all the neighbors in a line riding the waves of the pair potential $V(\mathbf{r})$, i.e., all of the distant neighbors sitting at the tops of the oscillations, an unfavorable position. That this interpretation is valid can be seen from the following expression of $D_{ij}^{(2)}(\mathbf{q})$ in terms of $V_{ind}(\mathbf{r})$

$$D_{ij}^{(2)}(\mathbf{q}) = \frac{2}{M} \sum_{n \neq 0} \nabla_i \nabla_j V_{ind}(\mathbf{X}_n) \sin^2 \left(\frac{\mathbf{q} \cdot \mathbf{X}_n}{2} \right).$$

Since $V_{ind}(\mathbf{r})$ has a period of $(\frac{1}{2}k_F)$ for large \mathbf{r} , values of \mathbf{q} for which $\mathbf{q} = \mathbf{K} + 2k_F$ will lead to a coherence between the $\sin^2[(\mathbf{q} \cdot \mathbf{X}_n)/2]$ term and the V_{ind} term, so that the sum will become anomalously large. This kind of instability is not a matter of nearest neighbors, as in solid He, *but is a question of the lattice structure as a whole*. Furthermore, it is clear that although the basic cause of the instabilities originates quite generally in the form of $F(\eta)$ in (II.15), the quantitative details are sensitive to which ϵ is used. Calculations show that using the RPA (Lindhard) dielectric function yield phonon spectra that are slightly more stable than those calculated with our form (II.14).

It is now easy to understand, at least qualitatively, the effect of self-consistency in the harmonic dynamical matrix [14]. The renormalized pair potential \tilde{V} going into $D_{ij,\sigma\sigma}(\mathbf{q})$ [given by (II.22)] is plotted for $Z = 1$ in Figure 5 for various values of the Gaussian width. Actually the pair potential, through the tensor $G_{ij}(n)$, depends on which two neighbors with separation \mathbf{X}_n are considered. We have plotted an 'average'

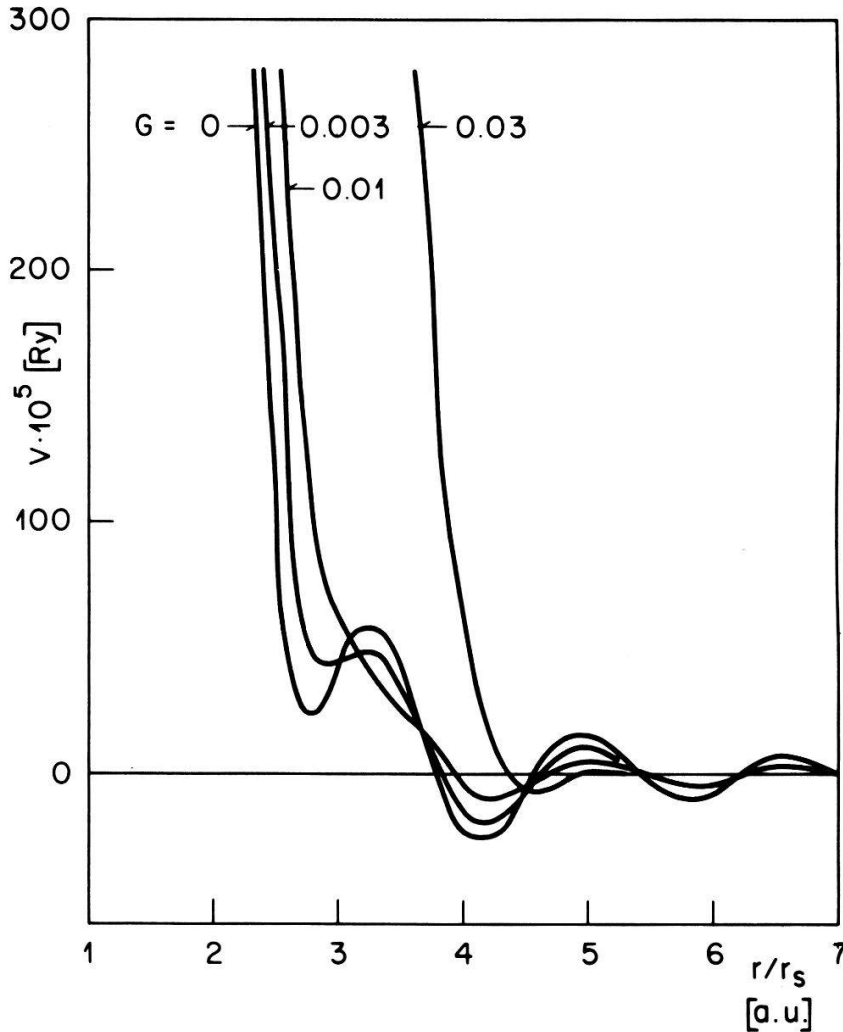


Figure 5
'Average' self-consistent pair potential $\tilde{V}(r)$ (see text), according to (II.22), for various values of G defined in (III.1).

self-consistent pair potential by replacing $G_{ij}(n)$ in (II.23) by its first part, the displacement auto-correlation function. This probably overestimates $G_{ij}(n)$. Putting

$$\langle U_i U_j \rangle = \delta_{ij} a_L^2 G, \quad (\text{III.1})$$

G is a measure of the main square deviation of an ion in units of the lattice constant squared. Several values of G have been chosen in plotting Figure 5. The general effect is clear: The finite Gaussian width tends to suppress the variation of $\epsilon(k)$ around $2k_F$ in (II.22) and the oscillations of $\tilde{V}(r)$ are weaker. Figure 3 does indeed show that Caron's [14] self-consistent phonon spectrum for FCC hydrogen at $r_s = 1.3$ is stable, while the harmonic spectrum is not stable. The Kohn anomalies are also present in Figure 3, and according to Caron, the self-consistent spectrum also shows an instability, but only at $r_s = 1.5$. In the light of our discussion we can safely conclude that self-consistent harmonic calculations will in general 'stabilize' a given lattice structure, since the Kohn anomalies are weakened.

Up to this point our conclusions have been based on the second-order dynamical matrix, (II.9) and (II.10). We have also performed third-order phonon calculations for hydrogen at several values of r_s . There is no *a priori* reason that third and higher-

order band-structure corrections should be small, but according to Ref. [8] the series (II.4) and (II.8) can be viewed as expansions in the parameter

$$\alpha \equiv \frac{V_{\mathbf{K}}}{\epsilon_{\mathbf{F}}} = \frac{4\pi e^2}{K^2 \Omega_c} \frac{2m}{k_{\mathbf{F}}^2},$$

where $V_{\mathbf{K}}$ is the Fourier component of the electron-ion potential for the smallest non-zero reciprocal lattice vector \mathbf{K} , and $\epsilon_{\mathbf{F}}$ represents the Fermi energy. For $r_s = 1.6$, α turns out to be about one-fifth for hydrogen. Our results in Figure 2 show that the third-order contributions are indeed small,

$$|D_{ij}^{(3)}| \ll |D_{ij}^{(2)}|.$$

However, when $D_{ij}^{(2)}$ itself is comparable in magnitude with the Coulomb part $D_{ij}^{(c)}$, so that the sum $D^{(2)}$ and $D^{(c)}$ is small (or even negative), the third-order term (II.16) can have a decisive influence on stability. Figure 2 shows that for $r_s = 1.0$ the harmonic spectrum including third order is unstable. Yet it was stable if only second order were included at this value of r_s . The location of the large Kohn anomaly is virtually unchanged by $D^{(3)}$ since the latter varies more smoothly with \mathbf{q} than its second-order counterpart. On the other hand, (II.16) shows that $D_{ij}^{(3)}$ grows as r_s^2 (the remaining factors in (II.16) depend only weakly on r_s) and thus becomes increasingly important for large r_s . For intermediate densities we can conclude that $D^{(4)}$ and higher-order terms should be of minor importance since they are again expected to be smaller than $D^{(3)}$.

Returning briefly to the question of static stability, we should mention how the behavior of $(1/\epsilon - 1)$ near $2k_{\mathbf{F}}$ affects the comparison of static energies between different structures. Brovman et al. [8, 9] examined various families of Bravais lattices, each family being parameterized by at least one variable (such as c/a). They find that for low pressure a family of trigonal structures has the lowest energy⁷⁾. Since the (static) second-order band-structure energy involves a sum over reciprocal lattice vectors of a summand proportional to $(1/\epsilon - 1)$, it was of interest to see to what extent Brovman's results could be understood in terms of the variation of ϵ near $2k_{\mathbf{F}}$. The favoring of very anisotropic structures (for larger r_s) can be understood simply in terms of this variation. A shell of \mathbf{K} vectors just inside the $2k_{\mathbf{F}}$ sphere is a very stable situation (low energy), whereas a shell just outside the sphere yields much higher (i.e., less negative) energy. This is really the same observation made by Ashcroft and Stroud [13], applied to metallic hydrogen.

It is not surprising that the static and dynamic stabilities are intimately connected. For the former is mirrored in the value of the elastic constants, which are negative for unstable structures [8], whereas the elastic constants are in turn related to the behavior of the phonon spectrum for small q . One has to be cautious, however, since for the purpose of calculating elastic constants to second order in V_{ep} from phonon frequencies one should in principle take into account $D^{(4)}$ for the latter [35, 36], which was not done here.

Finally we wish to comment on the validity of the adiabatic approximation. If the latter is questionable for any metal it would certainly be for metallic H, since the ratio

⁷⁾ Their results require careful interpretation, however, for they did not correct their third-order contributions to the energy for higher-order band-structure effects when the 3-pole expression became anomalously large. For the very anisotropic structures they propose this neglect may lead to some error, see Refs. [10] and [11].

of electron mass to ion mass is the largest here. We have evaluated the frequency-dependent ‘self-energy’ $D(\mathbf{q}\lambda, \Omega + i\delta)$ [see (II. 25)], for FCC hydrogen at various values of r_s . In order to obtain a frequency-dependent dielectric function the Lindhard expression (II. 15) was replaced by its dynamic counterpart, see Ref. [37] wherever it appeared in (II.14). This is the usual approximation for a frequency-dependent $\epsilon(k, \omega)$ of the ‘Hubbard type’ (II.14) [38]. Our results showed that the imaginary part $\Gamma(\mathbf{q}\lambda, \Omega)$ of D is roughly proportional to Ω . We can thus look for a pole of the phonon Green’s function (II.25) by solving

$$Z_0^2 = \bar{R}(\mathbf{q}\lambda) + 2iZ_0\gamma(\mathbf{q}\lambda) \quad (\text{III.2})$$

and identifying $Z_0 = X_0 + iY_0$ with a (complex) phonon frequency. Here \bar{R} is the real part R of D evaluated at X_0 and

$$\gamma(\mathbf{q}\lambda) = \Gamma(\mathbf{q}\lambda, \Omega)/2\Omega. \quad (\text{III.3})$$

A non-zero value of γ will in general lower the real part of Z_0 since

$$Z_0 = \pm(\bar{R} - \gamma^2)^{1/2} - i\gamma \quad (\text{III.4})$$

and thus make the phonons less stable, for the stability limit is reached when $\bar{R} = \gamma^2$. (For $\bar{R} - \gamma^2 < 0$, there would be exponentially growing lattice vibrations possible.)

Calculation shows that γ , as well as the difference between $R(\mathbf{q}\lambda, X_0)$ and $R(\mathbf{q}\lambda, 0)$, is generally quite small. Thus the frequency shift and damping due to a non-adiabatic treatment are negligible, except that very low frequencies may be pulled down to zero for a somewhat larger range of \mathbf{q} . (See Fig. 1b.)

IV. Conclusions

The purpose of this paper was two-fold: to unravel the origins of dynamic instabilities in Coulomb systems, and to assess the influence of corrections to the adiabatic, second-order, harmonic dynamical matrix. These corrections consist of including third-order band-structure terms in the dynamical matrix, taking into account a whole class of anharmonicities to obtain the ‘self-consistent harmonic’ dynamical matrix and evaluating a non-adiabatic harmonic dynamical matrix. We conclude:

(1) The dynamic instabilities (imaginary phonon frequencies) originate in strong Kohn anomalies. Therefore the relation between the $2k_F$ sphere and the reciprocal lattice is a good guide for studying the stability of a Coulomb metal. *The instability is not just a question of nearest neighbors, but involves the lattice structure as a whole.* The applications of these ideas to the investigation of the dynamics of H–He alloys will be pursued in a later work.

(2) The corrections to the adiabatic, harmonic, second-order dynamical matrix are not so important if the phonon frequencies are well-behaved (no modes with anomalously low or even imaginary frequencies). In this case, the corrections change the phonon frequencies quantitatively, but not qualitatively. When the frequencies are not well-behaved, and some lie anomalously low (as is the case even for some of the ‘most stable’ uniaxial lattices of Ref. [8]), the corrections have profound effects:

- a) The self-consistent harmonic treatment seems to raise the frequencies and so stabilize the lattice. It does so by weakening the Kohn anomalies.
- b) Third-order band-structure corrections seem to lower the frequencies. This was demonstrated for FCC hydrogen and is also true for magnesium [28].
- c) The adiabatic approximation seems to work well.

Acknowledgements

The authors are indebted to N. W. Ashcroft, J. Hammerberg and A. Baratoff for valuable discussions. One of us, H. Beck, acknowledges financial support from the 'Erziehungsrat des Kantons Zürich' during his stay at Cornell University where work on this subject began. We also thank the Swiss National Foundation which enabled us to continue the calculations while D. Straus was a guest at the University of Zurich.

REFERENCES

- [1] E. WIGNER and H. B. HUNTINGTON, *J. Chem. Phys.* **3**, 764 (1935).
- [2] F. V. GRIGOREW, S. B. KORMER, O. L. MIKHAILOVA, A. P. TOLOCHKO and V. D. URLIN, *ZhETF Pis. Red.* **16**, 286 (1972); *Engl. Transl. JETP Lett.* **16**, 201 (1972).
- [3] L. F. VERESHCHAGIN, to be published.
- [4] T. SCHNEIDER, *Helv. Phys. Acta* **42**, 957 (1969).
- [5] T. SCHNEIDER and E. STOLL, *Physica* **55**, 702 (1971).
- [6] T. SCHNEIDER and E. STOLL, *Helv. Phys. Acta* **43**, 453 (1970).
- [7] E. STOLL, P. F. MEIER and T. SCHNEIDER, *Nuovo Cimento* **23B**, 90 (1974).
- [8] E. G. BROVMAN, YU. KAGAN and A. KHOLAS, *Zh. Eksp. Teor. Fiz.* **61**, 2429 (1971); *Engl. Transl. Sov. Phys. JETP* **34**, 1300 (1972).
- [9] E. G. BROVMAN, YU. KAGAN and A. KHOLAS, *Zh. Eksp. Teor. Fiz.* **62**, 1492 (1972); *Engl. Transl. Sov. Phys. JETP* **35**, 783 (1972).
- [10] J. E. HAMMERBERG, Ph.D. Thesis, Laboratory of Atomic and Solid State Physics, Cornell University (Ithaca, N.Y.), January 1974.
- [11] J. E. HAMMERBERG and N. W. ASHCROFT, *Phys. Rev.* **B9**, 409 (1974).
- [12] W. HUME-ROTHERY, *The Metallic State* (Oxford University Press, London 1931).
- [13] D. STROUD and N. W. ASHCROFT, *J. Phys. F: Metal Physics* **1**, 113 (1971).
- [14] L. G. CARON, *Phys. Rev.* **B9**, 5025 (1974).
- [15] W. B. HUBBARD and R. SMOLUCHOWSKI, *Space Science Reviews* **14**, 599 (1973).
- [16] E. E. SALPETER, *Astrophys. J.* **181**, L83 (1973).
- [17] W. B. STRETT, *Astrophys. J.* **186**, 1107 (1973).
- [18] E. G. BROVMAN and YU. KAGAN, *Zh. Eksp. Teor. Fiz.* **52**, 557 (1967); *Engl. Transl. Sov. Phys. JETP* **25**, 365 (1967).
- [19] E. G. BROVMAN and YU. KAGAN, *Zh. Eksp. Teor. Fiz.* **57**, 1329 (1969); *Engl. Transl. Sov. Phys. JETP* **30**, 721 (1970).
- [20] P. P. EWALD, *Ann. Physik* **64**, 253 (1921).
- [21] E. W. KELLERMANN, *Phil. Trans. Roy. Soc. London* **A238**, 513 (1940).
- [22] C. B. CLARK, *Phys. Rev.* **109**, 1133 (1958).
- [23] J. HUBBARD, *Proc. Roy. Soc. (London)* **A243**, 336 (1957).
- [24] K. S. SINGWI, M. P. TOSI, R. H. LAND and A. SJOELANDER, *Phys. Rev.* **176**, 589 (1968).
- [25] K. S. SINGWI, A. SJOELANDER, M. P. TOSI and R. H. LAND, *Phys. Rev.* **B1**, 1044 (1970).
- [26] D. J. W. GELDART and J. H. VOSKO, *Can. J. Phys.* **44**, 2137 (1966).
- [27] P. NOZIERES and D. PINES, *Nuovo Cimento* **9**, 470 (1958); P. NOZIERES and D. PINES, *Phys. Rev.* **111**, 442 (1958); P. VASHISHTA and K. S. SIGWI, *Phys. Rev.* **B6**, 875 (1972).
- [28] E. G. BROVMAN, YU. KAGAN and A. KHOLAS, *Zh. Eksp. Teor. Fiz.* **61**, 737 (1971); *Engl. Transl. Sov. Phys. JETP* **34**, 394 (1972).
- [29] P. LLOYD, A. SHOLL, *J. Phys. C: Solid State Phys.* **1**, 1620 (1968).
- [30] N. S. GILLIS and T. R. KOEHLER, *Phys. Rev.* **B4**, 3971 (1971); **B5**, 1925 (1972).
- [31] G. BAYM, *Ann. Phys. (N.Y.)* **14**, 1 (1961).
- [32] N. R. WERTHAMER, *Am. J. Phys.* **37**, 763 (1969).
- [33] W. KOHN, *Phys. Rev. Letters* **2**, 393 (1959).
- [34] J. FRIEDEL, *Phil. Mag.* **43**, 153 (1952); *Adv. in Physics* **3**, 446 (1954); *Nuovo Cimento Suppl.* **2**, 287 (1958).
- [35] E. G. BROVMAN, YU. KAGAN and A. KHOLAS, *Zh. Eksp. Teor. Fiz.* **57**, 1635 (1969); *Engl. Transl. Sov. Phys. JETP* **30**, 883 (1970).
- [36] C. J. PETHICK, *Phys. Rev.* **B2**, 1789 (1970).
- [37] T. D. SCHULTZ, *Quantum Field Theory and the Many-Body Problem* (Gordon and Breach, New York and London 1964).
- [38] F. TOIGO and T. O. WOODRUFF, *Phys. Rev.* **B2**, 3958 (1970).

